Modelling arsenic(III) adsorption from water by sulfate-modified iron oxide-coated sand (SMIOCS)

Rakesh Chandra Vaishya and Sudhir Kumar Gupta*

Centre for Environmental Science and Engineering, Indian Institute of Technology, Bombay - 400076, India

Abstract: A medium developed by coating $BaSO_4$ and Fe on quartz sand known as sulfate-modified iron oxide-coated sand (SMIOCS) was evaluated for the removal of arsenic(III) from simulated water with an ionic strength of $0.01\,M$ $NaNO_3$ during batch studies. The medium was characterised for BET surface area, alkali-resistance, acid-resistance and the presence of iron and barium on the coated surface. Two simplified kinetic models, ie active available site (AAS) and chemical reaction rate models, were tested to investigate the adsorption mechanisms. The values of rate constants for both the models were found to decrease with increasing As(III) concentrations in the solute. The inverse relationship of rate constants of the reaction rate model with BET surface area showed that As(III) adsorption on SMIOCS was not due to physisorption but to chemisorption. A study of the effect of solute temperature showed that the adsorption of As(III) on SMIOCS media was due to chemisorption. The results of isothermal studies conducted at different pH values showed that adsorption data satisfied both the Langmuir and the Freundlich isotherm models. The adsorption of As(III) on the medium was pH dependent and maximum removal was observed in the pH range of 7–9.
© 2002 Society of Chemical Industry

Keywords: arsenic; chemisorption; coating; isotherms; kinetic model; quartz sand

NOTATION

b	Parameter for Langmuir equation $(dm^3\,mg^{-1})$, a constant related to energy and enthalpy of the system
C	Liquid-phase As(III) concentration at time t $(mg\,dm^{-3})$
C_c	Correlation coefficient
C_e	Liquid-phase As(III) concentration at equilibrium $(mg\,dm^{-3})$
C_o	Initial As(III) concentration in the aqueous phase $(mg\,dm^{-3})$
d_p	Particle diameter (mm)
K_F	Parameter of Freundlich equation $(mg\,g^{-1})\,(mg\,dm^{-3})^n$
K_R	Rate constant of reaction rate model $(dm^3\,mg^{-1}\,h^{-1})$
K_s	Rate constant for AAS model (h^{-1})
m	Dosage of SMIOCS medium $(g\,dm^{-3})$
n	Constant in the Freundlich equation
q_e	Amount of As(III) adsorbed at equilibrium $(mg\,g^{-1})$
Q_o	Amount of As(III) adsorbed corresponding to monolayer coverage $(mg\,g^{-1})$
t	Time (h)
Δq	Normalised standard deviation defined in eqn (5) (%)

INTRODUCTION

The presence of arsenic at elevated levels in drinking water supplies is of environmental concern because of its toxicity and adverse health effects on human beings. Recent epidemiological evidence on arsenic carcinogenicity suggests that the standard of $50\,\mu g\,dm^{-3}$ may not be sufficient to reduce the risk of cancer.[1] Therefore, USEPA is planning to enforce a standard in the range of 2–$20\,\mu g\,dm^{-3}$ for arsenic.[2] Chronic health effects of arsenic include development of various skin lesions such as hyperpigmentation (dark spots), hypopigmentation (white spots), and keratosis of hands and feet. Skin cancers and internal cancers (eg gall bladder cancer, lung cancer) can appear due to high arsenic exposure. Arsenic contamination has been, and continues to be, a specific problem of drinking water supplies in certain parts of Taiwan, Mexico, Chile and the Indian subcontinent.[3] Weathering of arsenic-bearing minerals and volcanic eruptions are major natural sources of arsenic contamination in the groundwater.

Among the treatment processes appropriate for removal of arsenic, adsorption by low cost adsorbents is considered to be less expensive than membrane separation and more versatile than ion exchange processes.[4] Innovative technology such as the coating of Fe oxides onto the surface of sand to effectively

remove/recover trace metals has been used by many researchers.[5] The results from their studies confirm that the utilisation of iron oxide-coated sand is worth developing for the removal of metal ions from water. This also offers a reliable and efficient removal process for complex inorganic and organic metals that may not be removed by conventional treatment methods.[6] Therefore, adsorption using low cost adsorbents such as oxide-coated sand could prove to be a suitable alternative. Ferrihydrite has been effectively used for the removal of arsenic from water and wastewater.[7] Arsenic was removed from groundwater in laboratory-scale studies using iron oxide-coated sand by various researchers.[8–10] Arsenate forms stable solids (ie $BaHAsO_4$ and $Ba_3(AsO_4)_2$) in the presence of Ba^{2+} at near neutral pH values in aqueous systems.[11] Arsenite has also shown strong affinity for sulfur. The removal of arsenic as orpiment or metal sulfides often occurs if hydrogen sulfide is present in water.[12] Therefore, if the coating on a sand surface is modified using Ba, Fe and S, arsenic removal by oxide-coated media may be enhanced with respect to Fe coating alone. Several models such as homogeneous surface diffusion, dual resistance mass transfer, and pore diffusion have been extensively applied to batch reactors to successfully describe the transport of molecules inside the adsorbent particles. The mathematical complexities of these models make them rather inconvenient for practical use.[13]

The aim of the present study was to examine the mechanism of adsorption of As(III) on sulfate-modified iron oxide-coated sand (SMIOCS) using simplified active available site (AAS) and reaction rate models. The research described here was designed to test the properties of SMIOCS as an adsorbent for As(III) removal in batch studies. The investigations also included isothermal studies conducted at different pH values with an analysis using both the Langmuir and the Freundlich isotherm models.

MATERIALS AND METHODS
SMIOCS preparation
The quartz sand used in this process was soaked in an acid solution (1.0 M HCl) for 24 h, rinsed with distilled water and dried at 105 °C. The geometric mean size of the sand was 498 μm. The coating was applied by taking 100 cm³ of 0.5 M $BaCl_2$ solution in a 1.0 dm³ glass beaker. To this solution, 12 cm³ of 2.5 M H_2SO_4 was added drop by drop with simultaneous shaking of the beaker till a dense white floc of $BaSO_4$ was formed. To this solution, 100 cm³ 0.5 M $Fe_2(NO_3)_3.9H_2O$ solutions were added and the mixture was shaken on a horizontal shaker at 30 strokes per minute for 10 min. Quartz sand (500 g) was added to this mixture and the mixture was mixed for an additional 30 min on a horizontal shaker. The beaker was then kept in an oven at 105 °C for 24 h. The coated sand was washed by distilled water till the supernatant liquid was clear. The washed sand was again kept in an oven to dry at 105 °C

for 20 h. This procedure yielded a slightly red-coloured sand.

Characterisation of SMIOCS
The total amount of iron coated on the sand surface, and its acid- and alkali-resistance were determined as per the method of Kuan *et al.*[14] The total amounts of barium and sulfur coated on the sand were determined by dissolving 5.0 g SMIOCS in 50 cm³ concentrated HNO_3 for 24 h. This was then filtered through 'Whatman 42' ashless filter paper and the filtrate was used to determine Fe, Ba and S by ICP-AES (model— 8440 Plasmalab; GBC, Australia). The surface areas of the quartz and coated sand were measured by the BET method using ASAP-2000 model (Micromeritics Corp, (USA). The pH_{zpc} of the media was determined by the potentiometric titration method described by Smith.[15]

Arsenic adsorption experiments
Batch adsorption kinetics
Batch sorption studies were carried out at room temperature 27 (±1) °C in an end-over-end rotary shaker at 44 ± 2 rpm. The SMIOCS dose was 20 g dm⁻³ (GM size = 498 μm) and the ionic strength of synthetic water was adjusted to 0.01 M with $NaNO_3$. The sorbate solution consisted of a total volume of 100 cm³ and 20 g dm⁻³ of media in 300 cm³ borosilicate glass bottles containing As(III) concentrations of 0.5, 1.0 and 2.0 mg dm⁻³ for kinetic studies. Stock As(III) solution was prepared by the dissolution of arsenic(III) oxide (As_2O_3) in distilled water. The desired initial pH of the solution was achieved by the addition of 0.1 M HCl or 0.1 M NaOH. The bottles were removed from the shaker after the desired contact time and the supernatant liquid was separated from the adsorbent by 'Whatman' filter paper No 42 (ashless) and the filtrate was stored at 2 °C until analysed for As(III) concentration.

Isotherm studies
The adsorption isotherms were obtained at different pH values and sorbate concentrations to determine the capacity of the medium for arsenic removal. The sorbate concentration was varied from 0.5 mg dm⁻³ to 3.5 mg dm⁻³, keeping the dose of sorbent at 20 g dm⁻³ in the solution and the ionic strength of synthetic water at 0.01 M with $NaNO_3$. The initial pH of the sorbate was adjusted before each experiment and the mixing time was 8 h. The pH drift during experimental studies was measured. The study was performed at room temperature 27 (±1) °C. Other procedures for sample handling were the same as for batch kinetic experiments.

Sample analysis
As(III) was determined as per the method of Johnson and Pilson.[16] The absorbance was measured at 865 nm by using a spectrophotometer (Spectronic 20 Genesys, USA). The minimum detection limit is 4 μg dm⁻³.

Samples were preserved using $1\,\mathrm{g\,dm^{-3}}$ ascorbic acid. All samples were analysed within 7 days of adsorption experiments.

KINETIC MODELS OF ADSORPTION
Active available site (AAS) model

The present coated sand surface may be considered to consist of a number of chemically active sites. The attachment of sorbate species occurs at these sites. So, the sorption capacity of sorbent for a specific sorbate is a function of 'available active sites' (AAS). The available sites can vary for the same sorbate–sorbent system under different environmental conditions such as pH, temperature, and particle size.

The attachment of arsenic species from aqueous phase to AAS can be considered to occur in two steps:

(i) transfer of sorbate from the aqueous phase to the AAS on the sorbent;
(ii) chemical complexation/ion-exchange at these chemically active sites.

The following assumptions were made in the development of the proposed AAS mass transfer model:

(i) both physisorption and chemisorption occur simultaneously;
(ii) the Langmuir isotherm model fits the sorption equilibrium data well.

The monolayer coverage parameter, Q_o, in the Langmuir isotherm model represents the saturation capacity of a sorbent. After derivation the linearised form of equation obtained is as follows.[17]

$$s\ln(C - C_e) + \ln C = (\ln C_o + s\ln(C_o - C_e)) + b\,K_s C_e t \quad (1)$$

where:

$$s = (-1 + bC_e) \quad (2)$$

The overall mass transfer coefficient can be determined using the Langmuir parameter (b), arsenic concentration (C) at time t and equilibrium arsenic concentration C_e. A plot of:

$$[s\ln(C - C_e) + \ln C] \qquad \text{versus } t$$

will yield a straight line of slope $K_s C_e b$, from which the overall mass transfer coefficient (K_s) can be obtained.[17]

Chemical reaction rate model

This model is based on mass law concept. The adsorption kinetics on oxide-coated sand may be treated as a chemical reaction. This equation may be represented by a second-order reaction of the form:

$$M + S \xrightarrow{K_R} [MS] \quad (3)$$

where M represents the dissolved metal contaminant, S the available surface sites, MS the adsorbed state, and K_R the reaction rate constant ($\mathrm{dm\,mg^{-1}\,h^{-1}}$). The rate equation is expressed in terms of concentrations of respective reactants. The rate constant, K_R, may be determined by least square linear regression of ln $[(C - C_e)/C]$ *versus t*. The slope of the line provides a value of $-K_R$. The linear form of this equation is:[18]

$$\ln\left(\frac{C - C_e}{C}\right) = -C_e K_R t + \ln\left(\frac{C_o - C_e}{C_o}\right) \quad (4)$$

The plot of ln $[(C - C_e)/C]$ *versus t* will give a straight line with slope of $-C_e K_R$ and intercept of $[(C_o - C_e)/C_o]$.

RESULTS AND DISCUSSION
Characteristics of media

The physical and chemical characteristics of plain quartz sand and sulfate-modified iron-oxide coated sand (SMIOCS) are shown in Table 1 which shows that the BET surface area of coated sand is nearly twice that of plain sand.

Time profiles of solute adsorption and test of kinetic models

The validity of the models discussed in this paper can be tested either by overlapping experimental data points with model points or by comparing quantita-

No	Characteristics	Plain sand	SMIOCS
1	Size[a]	$498\,\mu\mathrm{m}$	$\cong 498\,\mu\mathrm{m}$
2	Diameter of particle	$\cong 500\,\mu\mathrm{m}$	$\cong 500\,\mu\mathrm{m}$
3	Surface area BET ($\mathrm{m^2\,g^{-1}}$) size = 0.324 mm	–	7.9
4	Surface area BET ($\mathrm{m^2\,g^{-1}}$) size = 0.498 mm	1.79	3.74
5	Surface area BET ($\mathrm{m^2\,g^{-1}}$) size = 0.716 mm	–	2.95
6	Fe salt used for coating (%)	–	4
7	Total iron on coated sand ($\mathrm{mg\,g^{-1}}$)	–	5.31
8	Total barium on coated sand ($\mathrm{mg\,g^{-1}}$)	–	0.126
9	Total sulfur on coated sand ($\mathrm{mg\,g^{-1}}$)	–	0.47
10	Acid-resistance at pH $\cong$ 1.0 (%) [(dissolved Fe/total Fe) $\times$ 100]	0.02	45.67
11	Alkali-resistance at pH $\cong$ 12.67 (%) [(dissolved Fe/total Fe) $\times$ 100]	–	0.94
12	$\mathrm{pH_{zpc}}$	–	8.2

Table 1. Physical and chemical characteristics of plain sand and SMIOCS

[a] Except for BET surface area, all characteristics are for 0.498 mm-sized particles.

Table 2. Kinetic parameters and normalised standard deviations for As(III) adsorption on SMIOCS

Temperature $(K \pm 1)$	C_o $(mg\,dm^{-3})$	m $(g\,dm^{-3})$	d_p (mm)	Reaction rate model		Active available site (AAS) model	
				K_R $(mg\,dm^{-3}h^{-1})$	Δq (%)	K_s (h^{-1})	Δq (%)
300	0.5	20	0.498	3.45	33	1.47	31
300	1.0	20	0.498	2.4	18	1.42	13
300	2.0	20	0.498	0.83	5.76	1.10	4.0
300	1.0	20	0.324	4.78	70.0	0.68	62.0
300	1.0	20	0.716	7.18	16.0	1.59	15.0
300	1.0	10	0.498	1.55	0.75	1.27	0.75
300	1.0	15	0.498	1.88	2.56	1.47	2.0
303	1.0	20	0.498	1.59	6.4	1.34	2.28
313	1.0	20	0.498	1.68	8.5	1.36	7.74
323	1.0	20	0.498	1.54	6.93	1.26	5.25

tively by normalised standard deviation, Δq. The normalised standard deviation was calculated by the following equation:

$$\Delta q (\%) = 100 \times \sqrt{\frac{\sum \left[(q_{\exp} - q_{\text{cal}})/q_{\exp} \right]^2}{(n-1)}} \qquad (5)$$

where $q_{\exp}$ is solid phase loading data obtained experimentally at time t and q_{cal} is model calculated solid phase loading data at time t and n is the number of data points.

Effect of As(III) concentration
The kinetic parameters and normalised standard deviations values for the two models are presented in Table 2. Values of K_s and K_R were substituted in eqns (1) and (4) to get a series of sorption capacity (q) *versus* time profiles generated by AAS and reaction rate models respectively. Figures 1 and 2 present the model predicted sorption capacity (q) *versus* time profiles together with the experimental data for three initial As(III) concentrations for AAS and reaction rate models respectively. Based on Δq values (Table 1), it can be concluded that the AAS model gave a slightly better fit than the reaction rate model. Both K_s and K_R values were found to decrease with increasing As(III) concentrations from $0.5\,mg\,dm^{-3}$ to $2.0\,mg\,dm^{-3}$ in

the solute. These results are in accordance with the assumptions made in the AAS model that there are limited numbers of chemical sites on which sorption can take place. Reduced values of K_s and K_R at higher concentrations were due to fewer active available sites for sorption/reaction. Table 2 also shows higher values of normalised standard deviation values for initial As(III) concentration of $0.5\,mg\,dm^{-3}$ as compared with the other two concentrations. More availability of active available surface sites in solute for initial As(III) concentration of $0.5\,mg\,dm^{-3}$ may be the reason for such results. The linearised K_R and C_o values on a log-log plot showed a correlation coefficient of 0.94 whereas the correlation coefficient was 0.84 for K_s and C_o values. The following relationships were obtained between mass transfer rates and C_o values:

$$K_R = 1.90\, C_o^{-1.0277} \qquad (6)$$

$$K_s = 1.32\, C_o^{-0.2092} \qquad (7)$$

High correlation coefficients ($r^2 > 0.83$) support the assumptions related to monolayer coverage of metal on the surface.

Effect of sorbent dose
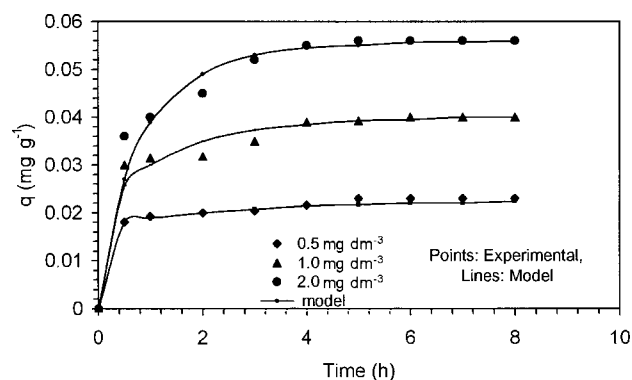From Table 2 it can be seen that values of K_s and K_R

Figure 1. Fitting of AAS model for As(III) adsorption onto SMIOCS at different initial As(III) concentrations.
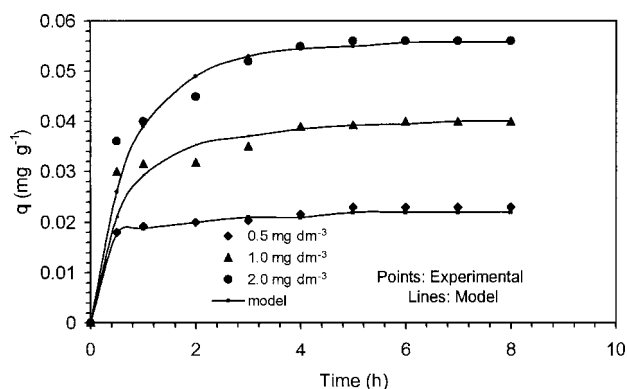

Figure 2. Fitting of reaction rate model for As(III) adsorption onto SMIOCS at different initial As(III) concentrations.

were found to increase with an increase in the amount of sorbent in the solution. There was almost a linear relationship between K_R values and dose of sorbent whereas this linear relationship was lacking in the AAS model at higher doses. Although both models gave a good fit for all three sorbent doses, if comparisons are made based on Δq values then the AAS model was a better fit than the reaction rate model. With increasing sorbent dose from 10 to 20 g dm^{-3} the adsorption of As(III) per unit mass of adsorbent decreased. This sorbent concentration effect can be explained by two theories. According to the first theory at a higher dose adsorption sites remain unsaturated during adsorption reaction, resulting in lower adsorptive capacity utilisation of the adsorbent.[19] As per the second theory, aggregation/agglomeration of sorbent particles at a higher dose may decrease the surface area and increase the diffusional path length. The ability of the reaction rate model to predict the sorption kinetics, both at lower as well as higher sorbent doses indicated the validity of the concept of chemical sites available for reaction. The variation in K_R with sorbent dose m is presented in Fig 3 for the reaction rate model. The values of K_R varied linearly with sorbent dose ($C_c = 0.98$).

Effect of media size

Table 2 also illustrates that both K_s and K_R varied with media size for the same dose of media and initial As(III) concentration. No linear relationship can be established with K_R values and sorbent sizes. It indicates that K_R was relatively independent of particle size. Furusawa and Smith[20] have also observed that the mass transfer coefficient was indeed independent of particle size. However, there was some linear relationship with K_s values for different size of media. An increase in K_s values was observed with an increase in media size from 0.324 mm to 0.716 mm. Therefore, unlike the reaction rate model, the AAS model was influenced by the size of particles. Table 2 also shows very high values of normalised standard deviations for both the models for 0.324 mm sized particles. The results show that sorbate–sorbent affinity for this size of media was much higher than the other two sizes. It
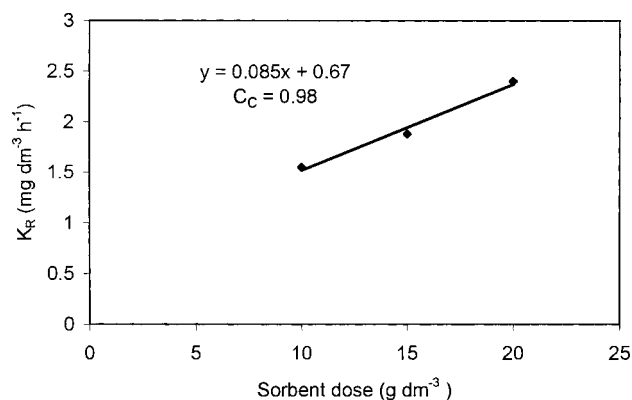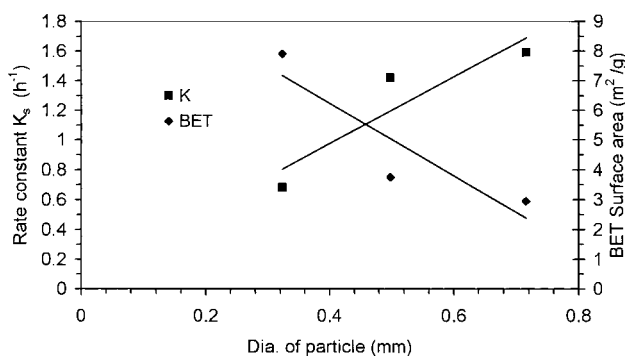

Figure 4. Plot for variation of BET and AAS constant with respect to diameter of particle.

could be due to better coating and more BET surface area (Table 1) of this size of media.

Variations in K_s with media size (d_p) and BET surface area are presented in Fig 4. With limited data (only three particle sizes) it can be seen from Fig 4 that there was an inverse linear relationship between BET surface area and K_s. The coefficient of correlation was 0.82. The media size (d) showed an almost linear relationship with K_s values ($C_c = 0.84$). The inverse relationship of K_s with BET surface area showed that As(III) adsorption on SMIOCS was not due to physisorption but due to chemisorption. The results of this limited study showed that the BET surface area was not an effective criteria for relating As(III) adsorption on sulfate-modified iron oxide-coated sand.

Effect of solute temperature

The effect of solute temperature on As(III) removal by SMIOCS was studied at pH 7.2 and at 0.01 M NaNO$_3$ ionic strength. The temperature variation studies were necessary to investigate the dissolution of Fe and Mn from coated media because these media were subjected to heating in an oven during coating. Although the effect of temperature was marginal for As(III) removal, this study showed that solute temperature had a linear relationship with the capacity of media. The kinetics of uptake of As(III) by SMIOCS was also investigated at three different temperatures, ie 30, 40 and 50 °C. Table 2 also presents K_s and K_R values at different temperatures along with normalised standard deviations ($\Delta q\%$). Based on Δq values it was concluded that the AAS model was a better fit than the reaction rate model (Fig 5). The K_s values were calculated using the Langmuir parameter b from isothermal data generated at the same temperatures. Both K_s and K_R values increased with an increase in temperature from 30 to 40 °C whereas K_s and K_R values decreased when the temperature was increased from 40 to 50 °C. This may be due to dissolution of adsorbing species and availability of more active surface centres for adsorption. Findings also clearly indicated that solute temperatures above 40 °C favoured As(III) adsorption on SMIOCS but more removal may be due to co-precipitation rather than adsorption. It supported the
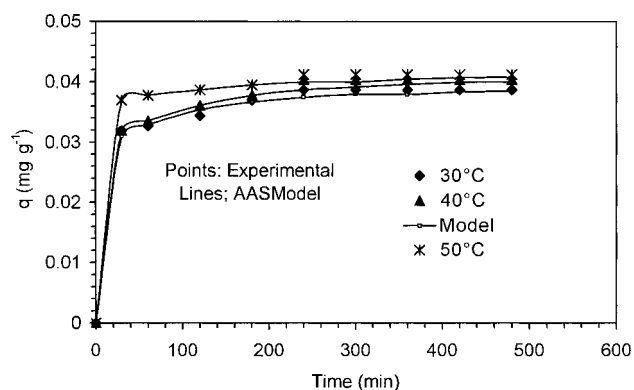

Figure 3. Effect of adsorbent dose on reaction rate model constant.

Figure 5. Fitting of AAS model for As(III) adsorption onto SMIOCS at different solute temperatures.

Figure 6. Adsorption isotherms for As(III) on SMIOCS at different pH values, adsorbent dose=20 g dm^{-3}: lines are Freundlich model curves.

assumption made in the development of the AAS model that K_s can qualify for the chemisorption-type interactions as K_s responded to the change in temperature of the reaction mixture.

The fitting parameters for the Langmuir and the Freundlich isotherms based on isothermal studies are shown in Table 3. It can be seen that the slope '$1/n$', which reflects the intensity of adsorption, increases with increasing temperature of the solute. These results are similar to observations reported by Machesky.[21] According to him, the metal cation adsorption increases with increasing temperature. The relationship between adsorption capacity (Q_o) based on the Langmuir isotherm and temperature (K) can be represented by the following equation:

$$Q_o = 0.001 \times (K) - 0.195 \qquad (8)$$

The enthalpy of adsorption was determined by relating the Langmuir capacity factor, $Q_M(=bQ_o)$ to the temperature variation.[22] The internal energy, $-\Delta U_o$, was determined from the slope of Q_M versus $1/T$ (figure not shown here) using van't Hoff's equation. The enthalpy of adsorption (ΔH_o) can be calculated using the following relationship:

$$\Delta H_o = -\Delta U_o + RT \qquad (9)$$

The value of the enthalpy of adsorption (ΔH_o) for the sorption of As(III) by SMIOCS was -7.49 kJ mol^{-1} at 27 °C. The negative value of the enthalpy of adsorption suggests that the adsorption process is exothermic in nature.
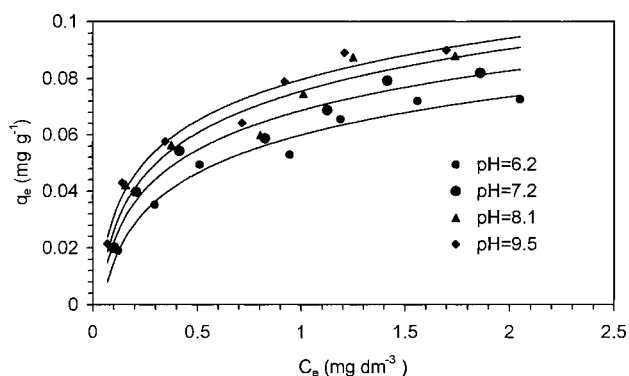
Equilibrium studies

Figure 6 presents the Freundlich model curves at different pH values and room temperature 27 ($\pm$ 1) °C for the adsorption of As(III) by SMIOCS media. The experimental data were fitted to both the Freundlich and the Langmuir isotherms. The isotherm parameters for both models are presented in Table 3. The data and their accompanying Freundlich model curves illustrate an increase in adsorption capacities with an increase in initial solution pH till it reaches a plateau for As(III) adsorption on SMIOCS. The present experimental equilibrium relationships could also be described quite well by the Langmuir isotherm model ($C_c > 0.95$). Matis et al[23] have also reported that sorption of anions is typically pseudo-Langmurian for all sorbate–sorbent ratios, indicating one dominant type of binding site, that of ligand exchange. The polynomial regression was applied to develop the relationship between the Langmuir monolayer capacity, Q_o, and pH values. The fitted polynomial equation ($C_c > 0.99$) is as follows:

$$Q_o = -0.0017 \times \text{pH}^2 + 0.0308 \times \text{pH} - 0.0371 \qquad (10)$$

Figure 7 depicts the effect of pH on the removal of As(III) by SMIOCS. The removal of As(III) increases as the pH of the system increases till it reaches a maximum at about pH $\cong$ 9.2. It is noteworthy that at this pH arsenite (H_3AsO_3) starts dissociating ($pK_a = 9.2$) to form $H_2AsO_3^-$. The result can be interpreted with the help of the pH$_{zpc}$ of the media (Table 1).

Table 3. Langmuir and Freundlich isotherm constants for As(III) adsorption on SMIOCS at different temperatures and pH values (media size=0.498 mm)

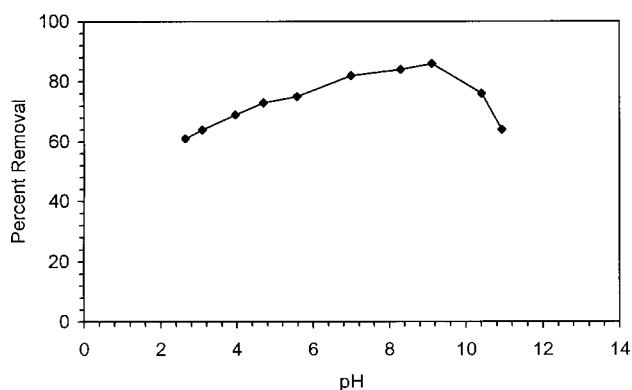| Variable		Langmuir model constants			Freundlich model constants		
Temp (K $\pm$ 1)	pH	Q_o (mg g^{-1})	b (dm^{3}g^{-1})	C_c	K_F [mg$^{n-1/n}$ g^{-1} (dm^3) 1^n]	$1/n$	C_c
300	6.2	0.09	2.13	0.98	0.058	0.468	0.96
300	7.2	0.096	3.06	0.98	0.067	0.442	0.92
300	8.1	0.104	2.84	0.96	0.075	0.438	0.90
300	9.5	0.104	3.63	0.98	0.08	0.416	0.93
303	7.2	0.122	2.27	0.90	0.08	0.42	0.96
313	7.2	0.136	1.91	0.92	0.084	0.5	0.97
323	7.2	0.143	1.71	0.94	0.089	0.56	0.90

Figure 7. Effect of pH on As(III) adsorption on SMIOCS.

Below pH_{zpc} (8.2), the media surface is positively charged and in this pH range arsenite is available as the neutral H_3AsO_3 species.[24] Therefore, only physical adsorption driving (Van der Waals') forces between H_3AsO_3 and SMIOCS are present, resulting in less adsorption. Also in the acidic pH range the net release of H^+ ions blocks the surface sites available for sorption as iron-based sorbents have shown high sorption capacity for cations.[6]

At near neutral pH values (7–9), slow dissociation of weak arsenic acid (H_3AsO_3) produces arsenite ion ($H_2AsO_3^-$). This partially neutral and partially negative charged arsenite ion is attracted to the positively charged (below pH 8.2) surface of SMIOCS, resulting in high As(III) removal in this range. It may be hypothesised that in the pH range of 7–9, the removal of arsenic(III) may be due to combination of electrostatic attraction between As(III) and media and Van der Waals, attraction with the possibility of the former dominating. When the pH was greater than 8.2, ie pH_{zpc} of media, the surface of the medium becomes negatively charged. It is possible that Na^+ cations were attracted to the negatively charged surface species and provided charge compensation. Experimental results of ionic strength variation also showed that when the ionic strength of the solution was increased from $0.001\,M$ to $0.1\,M$ $NaNO_3$, As(III) removal increased slightly (Vaishya and Gupta, unpublished).

The decrease in As(III) removal by SMIOCS in the pH range of 9.5–12 may be the result of net negative charge on SMIOCS media ($>pH_{zpc}$). The dominant species of arsenite in this pH range are $HAsO_3^{-2}$ and $HAsO_3^{-1}$, which are not favourable for adsorption on the media's surface. Manning and Goldberg[25] also reported maximum adsorption in the pH range of 7.5–9.5 for As(III) adsorption on kaolinite, illite, montmorillonite and amorphous aluminium hydroxide.

CONCLUSIONS

The active available site (AAS) and reaction rate models can successfully describe the As(III) adsorption onto SMIOCS under different experimental conditions. Both the models predicted that the adsorption process was due to chemisorption. Both the Langmuir and the Freundlich isotherm equations were able to describe the partitioning behaviour of the system at different pH values. The adsorption of As(III) on SMIOCS was pH dependent and the pH adsorption edge data showed that As(III) removal was optimum in the pH range of 7–9.

REFERENCES

1 Smith AH, Hopenhayn-Rich C, Bates MN, Goeden MM, Hertz-Picciotto I and Duggan H, Cancer risks from arsenic in drinking water. *Envir Health Perspectives* **97**:259–267 (1992).
2 Pointius FW, Crafting a new arsenic rule. *J Am Water Works Assoc* **86**:6–10 (1994).
3 Karim MM, Arsenic in groundwater and health problems in Bangladesh. *Water Res* **34**:304–310 (2000).
4 Chen HW, Frey MM, Clifford D, McNeill LS and Edward M, Arsenic treatment considerations. *J AWWA* **91**:74–85 (1999).
5 Edward MA and Benjamin MM, Adsorptive filtration using coated sand: a new approach for treatment of metal bearing wastes. *J Water Pollution Control Fed* **61**:1523–1533 (1989).
6 Benjamin MM, Slatten RS, Bailey RP and Bennett T, Sorption and filtration of metals using iron-oxide-coated sand. *Water Res* **30**:2609–2620 (1996).
7 Pierce ML and Moore CB, Adsorption of arsenite and arsenate on amorphous iron hydroxide. *Water Res* **16**:1247–1253 (1982).
8 Joshi A and Chaudhuri M, Removal of arsenic from ground water by iron oxide coated sand. *J Environ Engg ASCE* **122**:769–771 (1996).
9 Thirunavukkarasu OS, Viraraghavan T and Subramanian KS, Removal of arsenic in drinking water by iron oxide coated sand and ferrihydrite—batch studies. *Water Qual Res J Canada* **36**:55–70 (2001).
10 Vaishya RC and Gupta SK, Arsenic (III) contaminated groundwater treatment by iron oxide coated sand (IOCS) media, In *Proceedings of International Conference on Civil Engineering – 2001 Vol II*, July 23–25, 2001, Banglore, India. pp 764–770 (2001).
11 Robin R, The solubility of barium arsenates: Sherritt's barium arsenate process. *Metallurgical Trans* **16B**:404–406 (1985).
12 Hounslow AW, Groundwater geochemistry: arsenic in land fills. *Groundwater* **18**:331–333 (1980).
13 Ho YS and McKay G, A comparison of chemisorption kinetic models applied to pollutant removal on various sorbents. *Trans Inst Chem Engng* **76B**:1–10 (1998).
14 Kuan WH, Lo SH, Wang MK and Lin CF, Removal of Se(IV) and Se(VI) from water by aluminum oxide-coated sand. *Water Res* **32**:915–923 (1998).
15 Smith EH, Surface complexation modeling of metal removal by recycled iron sorbent. *J Environ Engg ASCE* **124**:913–920 (1998).
16 Johnson DL and Pilson MEQ, Spectrophotometric determination of arsenite, arsenate, and phosphate in natural waters. *Anal Chim Acta* **58**:289–299 (1972).
17 Mittal AK, Biosorption of cationic dyes by dead macro fungus: *Fomitopsis carnea*, *PhD thesis*, Indian Institute of Technology, Bombay (1996).
18 Smith EH, Modeling batch kinetics of cadmium removal by a recycled iron adsorbent. *Separation Science and Technology* **33**:149–168 (1998).
19 Honeyman BD and Santschi AH, Metals in aquatic systems. *Environ Sci Technol* **22**:862–869 (1988).
20 Furusawa T and Smith JM, Fluid–particle and intra-particle mass transport in slurries. *Ind Eng Chem Fundm* **12**:197–203 (1973).
21 Machesky ML, In *Chemical Modeling of Aqueous Systems II*, Ed by Melchor DC and Bassett RL, American Chemical Society

Symposium Series 416, American Chemical Society, Washington DC. pp 282–292 (1990).

22 Cavelcante CL and Ruthven DM, Adsorption of branched and cyclic parafins in silicate. 1. equilibrium. *Ind Eng Chem Res* **34**:177 (1995).

23 Matis KA, Zouboulis AI, Zamboulis D and Valtadorou AV, Sorption of As(V) by goethite particles and study of their flocculation. *Water, Air and Soil Pollution* **111**:297–316 (1999).

24 Gupta SK and Chen KY, Arsenic removal by adsorption. *J Water Pollution Control Fed* **50**:493–506 (1978).

25 Manning BA and Goldberg S, Adsorption and stability of arsenic (III) at the clay mineral–water interface. *Environ Sci Technol* **31**:2005–2011 (1997).